

See discussions, stats, and author profiles for this publication at: <https://www.researchgate.net/publication/231632243>

Interactions between Thiol Molecular Linkers and the Au₁₃ Nanoparticle

ARTICLE *in* THE JOURNAL OF PHYSICAL CHEMISTRY B · MAY 2002

Impact Factor: 3.3 · DOI: 10.1021/jp014483k

CITATIONS

64

READS

41

3 AUTHORS, INCLUDING:



Andreas Larsson

Luleå University of Technology

56 PUBLICATIONS 996 CITATIONS

SEE PROFILE



Michael Nolan

University College Cork

88 PUBLICATIONS 2,366 CITATIONS

SEE PROFILE

Interactions between Thiol Molecular Linkers and the Au₁₃ Nanoparticle

J. A. Larsson,* M. Nolan, and J. C. Greer

NMRC, Lee Maltings, Prospect Row, Cork, Ireland

Received: December 10, 2001; In Final Form: April 3, 2002

The structure and binding of thiol molecular linkers to gold surfaces and nanoparticles is central to the understanding of the electronic properties of self-assembled monolayers and, of relevance to recent studies, to nanoscale assemblages consisting of molecular wires and metal nanoparticles. The study of mono-molecular electron transport generally requires consideration of bonding with irregular metallic contacts or poorly defined surfaces such as break junctions, electromigration generated gaps, and scanning probe microscopy tips. These structures can locally bear a closer resemblance to atomic clusters, as compared to neat metallic surfaces. It has also emerged that the prediction and understanding of the electronic transport properties for molecular wires and nanoscale assemblies requires detailed knowledge of thiolate–gold cluster interactions. Recent debate has focused on the nature of the thiolate bonding to surfaces, and the effect of disordering and distortion in gold cluster structures on thiolate bonding. We apply density functional theory methods to study the interactions of two thiols—methanethiol and benzenethiol—with Au₁₃, a gold “magic” number cluster. Our study emphasizes the effects of thiolate bonding on the electronic structure of the linker molecule and gold cluster. We find significant local distortion of the gold cluster upon bonding to a thiol group, resulting in modifications to the electronic structure of the complex. Consideration of a finite gold cluster avoids many of the issues related to thiolate bonding on gold surfaces, and allows us to assess the impact of bonding to gold nanoparticles in terms of electronic structure. We discuss our findings in relation to electron transport properties in self-assembled systems.

1. Introduction

Self-assembly of organic molecules onto metal surfaces and nanoparticles via thiol groups is an area of importance to molecular electronics and for biotechnology applications. Electronic transport across molecules is being explored^{1–3} to assess the properties of nanowires, and to investigate electron transfer at metal–molecule interfaces. Previous quantum chemical calculations have addressed the issue of the bonding configurations of thiolate molecules on gold surfaces;^{4–8} the resulting electronic structure and the impact on electronic transport properties have also been explored to a limited extent.⁴

In this work, we consider the structures of methanethiolate–Au₁₃ and benzenethiolate–Au₁₃ and the impact of bonding on the electronic structure of the complexes. We discuss our findings in relation to studies of thiolate bonding to gold surfaces and thiolate bonding to larger ordered and disordered clusters. We have studied methanethiol to determine the nature of thiolate bonding to the $n = 13$ “magic number” gold cluster, and then proceed to discuss our results in light of previous studies of methanethiol bonded to surfaces and larger gold clusters, in particular recent studies of the Au₃₈ cluster.^{9,10} Surface studies of thiolate bonding have primarily concentrated on the Au(111) surface using either periodic boundary condition slab models,^{7,8} or cluster models designed to model surface properties.^{4–6} Related studies have focused on larger gold clusters stabilized by thiolates, and the effect of order/disorder on the geometries at the thiolate-stabilized cluster surface.^{9,10} By considering a smaller magic number ($n = 13$) cluster, we avoid issues relating to the ordered/disordered configurations that are formed for larger clusters. Although several energetically competing iso-

mers have been found for Au₁₃¹⁰ using analytical potentials and genetic search methods, the structures containing thirteen gold atoms display a high degree of symmetry. We chose the octahedral, lowest energy structure of the Au₁₃ cluster¹¹ as determined from density functional calculations, both within the local density approximation and when applying gradient corrections to the exchange–correlation potential. This choice of metallic cluster in turn allows us to: (a) directly examine the role of single thiolate bonding to the gold cluster surface, (b) identify the accompanying geometric distortions of the cluster, and (c) assess the impact of bonding upon the electronic structure of the moiety. We have also studied benzenethiol as a ligand, both in its role as a prototype for molecular electronic transport studies and to examine effects associated with π -conjugation in molecular wires upon bonding, and as well to gauge the effect of the bonding on the geometry of a molecular wire.

2. Background

Previous theoretical studies of thiolate bonding to gold surfaces^{4–8} have focused upon the possible bonding configurations on the (111) and (100) surfaces, with the majority of these studies focusing on the (111) surface. Calculations of larger gold clusters, particularly Au₃₈, have considered the role of the cluster geometry and thiolate bonding in terms of structure stability.^{9,10}

In an early work, Sellers et al.⁴ have investigated the geometry of methanethiolate–gold (100) and (111) surfaces, and have considered the resulting electronic structure of the thiolate–gold bond using Hartree–Fock theory and second–order many-body perturbation theory (MBPT2). These authors use a finite cluster model to simulate the gold surfaces. Geometry optimization was confined to the molecular part of the metal–molecule

* Corresponding author.

complex, with all other degrees of freedom constrained. Their calculations indicate that the hollow site is favored for bonding, but that relatively low transition barriers exist between neighboring bonding sites. Using density functional theory with a gradient corrected exchange correlation potential, Beardmore et al.⁵ studied methanethiolate bonding on the Au(111) surface, again with finite cluster models used to represent the gold surface. In their study, the position of the molecule on the surface was optimized and all other degrees of freedom were held fixed. They found that the bridge, face-centered cubic (fcc), and hexagonal close-packed (hcp) site (the latter two sites correspond to hollow sites with differing atomic configurations below the surface plane) are nearly isoenergetic. Grönbeck et al.⁷ have presented periodic boundary condition slab calculations for methanethiolate bonded to the gold (111) surface, using gradient corrected density functional theory. They find the hcp hollow site to be much more stable than other sites considered. Akinaga et al.⁸ have also considered methanethiolate bonding to a cluster model of the Au (111) surface, by applying density functional theory with relativistic corrections using cluster models of the gold surfaces, and find the bridge and fcc hollow site to be close in energy. In that work, Hayashi et al. are reported to obtain comparable results using methods similar to those of Akinaga et al.

Johansson et al.⁶ have considered the bonding of benzene-thiolate to Au(111) using Hartree–Fock theory and a 10 atom cluster to model the gold surface. They find the hcp hollow site to be energetically the most favorable. Yaliraki et al. have considered benzene–dithiol bonding between two metallic contacts in the context of molecular conductance³. Within a Hartree–Fock approach, they have considered bonding to hcp hollow and atop sites onto gold (111) contacts and the corresponding impact of bonding on molecular conductance.

Häkkinen et al. have considered charge distributions, density of states, charging energies, and ionization potentials of a truncated octahedral fcc Au₃₈ cluster passivated by twenty-four methanethiolate molecules.⁹ Garzón et al. have questioned these results on the basis that the gold cluster geometry used does not correspond to an energy minimum. They find a disordered Au₃₈ geometry and an increase in surface disorder as the cluster is passivated by thiols.¹⁰

Of relevance to molecular electronics is the alignment of the molecular and metal contact energy levels. The alignment of metal states relative to molecular orbitals determines electron injection properties, and this alignment has only begun to be investigated in the literature.^{3,12}

From the above discussion, it is clear that basic questions concerning thiolate bonding to gold surfaces and gold clusters remain topical. In the following, we present results that yield new information for the bonding of molecular wires to small gold clusters, and as well, present a detailed analysis of orbital alignment and mixing between the molecular wire and gold cluster. We study the bonding of thiols to a small gold cluster to mimic the situation for bonding of thiols to irregular metallic contacts and poorly defined surfaces such as break junctions, electromigration generated gaps, and scanning probe microscopy tips. We find that thiol bonding to small gold clusters is, in principle, still quite similar to that found for bonding to bulk surfaces. The discrepancies found between previous studies for the bonding of thiols to clusters and slabs is attributed, not to differing chemical bonding, but to geometrical constraints imposed in previous studies. Our results with a small gold cluster and no geometry constraints correlate well to the slab study of Grönbeck et al.⁷ for bond distortions.

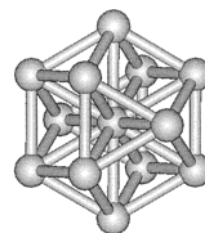


Figure 1. Molecular structure of the Au₁₃ cluster in octahedral (O_h) symmetry. The bond distances from the central gold atom to a surface atom is 2.929 Å and between two neighboring surface gold atoms is 2.929 Å.

3. Methods

All calculations have been performed within the density functional theory using the B3-LYP exchange-correlation functional^{13,14} as implemented in the Turbomole program system.¹⁵ Grönbeck et al. concluded that the PBE exchange-correlation functional is best suited for treatment of the gold surface.⁷ However, the Au₁₃ cluster and the thiolate–Au₁₃ complexes studied in this work have substantial molecular character. In ref 16, it was shown that the B3-LYP functional yields more accurate results for molecular systems; the B3-LYP functional was thus chosen over the PBE functional. All cluster and molecular structures reported are a result of geometry optimizations with symmetry constraints imposed (full geometry optimization). A sixty-electron relativistic effective core potential (RECP)¹⁷ has been used to describe the gold atom core electrons. The nineteen valence electrons of the gold atoms are explicitly treated using a polarized valence double- ζ basis set allowing the effect of the gold 5s, 5p, 5d, and 6s electron interactions to be included within the computations. Full geometry optimization for the individual thiol molecules was performed using a valence double- ζ polarized basis set (DZVP).¹⁸ Methanethiol was geometry optimized in C_{3v} symmetry, and benzenethiol was optimized within C_s symmetry. The Au₁₃ cluster was geometry optimized in O_h symmetry, as the lowest energy structure is found to be octahedral in ab initio calculations,¹¹ in contrast to analytical potential energy studies.¹⁰ The octahedral structure consists of faces composed of either four atoms or three atoms. As the octahedral cluster corresponds to gold's bulk symmetry and may be constructed by cleaving along (100) and (111) planes (see Figure 1), we denote the resulting cluster surface configurations as the (100) and (111) faces for the four- and three-atom faces, respectively. To study the metal–molecule interaction, bonding to the (111) and (100) cluster faces was investigated, corresponding to the (hcp) hollow site, and the hollow site bonding on the (111) and (100) surfaces, respectively. In addition a bonding configuration with resemblance to the bridge site on a (111) surface, in which the sulfur atom is bonded to two gold atoms, was investigated. The atop bonding site, in which the sulfur atom is bonded to only one apex gold atom, was not considered, as previous studies have shown this bonding configuration to be significantly higher in energy than the (hcp) hollow site bonding configuration.^{3–5,8}

4. Results and Discussion

4.1. Methanethiolate–Au₁₃. Full optimization of the geometry of both the (111) hollow-site (in C_{3v} symmetry) and the bridge site (in C_s symmetry) bonding configurations and the (100) hollow site (in C_s symmetry) bonding configuration of methanethiolate–Au₁₃ were performed. Bonding to the (111) bridge site and the (100) hollow site causes the metal cluster to become extremely distorted during the geometry optimization

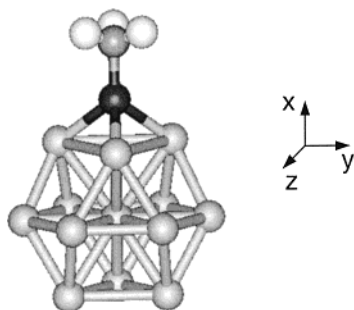


Figure 2. Molecular structure of the (111) bonding configuration of methanethiolate-Au₁₃ in C_{3v} symmetry.

procedure and form exotic higher energy configurations. Through geometry relaxations in different symmetries and starting from different initial geometries for the thiolate, we conclude the bonding to the (111) hollow-site to be the most stable configuration.

4.1.1 Bonding Configurations. For the minimum energy configuration, the sulfur atom is bonded at a hollow site in C_{3v} symmetry, as depicted in Figure 2. A vibrational calculation using Hartree-Fock theory has confirmed that this is a true local minimum. The angle formed by the sulfur-carbon bond with the gold surface is 180° . The optimized bond lengths are as follows: the sulfur atom is bonded to three of the gold atoms that form a (111) facet. The sulfur-gold bond distance is 2.551 Å. For the bonded thiolate molecule, the sulfur-carbon bond length is 1.840 Å and the carbon-hydrogen bond distances are 1.098 Å. The distance from the gold atoms bonded to sulfur to the cluster's central gold atom is 3.132 Å, which is 0.203 Å (6.9%) longer than for the bare gold cluster. Notably, the bond distances between the gold atoms forming the (111) facet to which the thiolate is bonded (henceforth referred to as the bonding gold atoms) are 3.622 Å, representing a large bond stretch of 0.693 Å (24%) relative to the bare gold cluster. The bond lengths between the central cluster gold atom to the gold atoms not bonded to the thiolate molecule are not significantly distorted as compared to the bare gold cluster. It is clear that the thiolate-gold bond introduces substantial local atomic rearrangement. The structural relaxation is quite independent of the long-range order/disorder of the bare metal cluster—although clearly a disordered metal cluster is capable of providing differing bonding sites for the thiolates.

4.1.2. Electronic Structure. To analyze the electronic structure of the complex, the energy levels for the gold atom, gold cluster, methanethiol molecule, and the methanethiolate-Au₁₃ complex are shown in Figure 3. To aid in the interpretation of the resulting single particle spectra, the parentage of the energy levels are traced by the contribution of individual atomic orbitals within a given molecular orbital, and are shown in Table 1. Inspection of Figure 3 reveals that the HOMO and LUMO energy levels are predominantly constructed from gold orbital contributions, specifically from the gold cluster HOMO and LUMO arising from the gold 6s bands. The energy difference between the highest occupied and lowest unoccupied (HOMO-LUMO gap) molecular orbitals of the methanethiolate-Au₁₃ complex is 2.03 eV. The HOMO and LUMO levels of methanethiol lie at -6.20 eV and 0.74 eV, respectively, whereas the HOMO level for octahedral Au₁₃ lies at -4.85 eV. There are minor sulfur contributions to the HOMO level from the sulfur 3p_z orbital, and to the LUMO level from the sulfur 3s orbital.

From Table 1, it is seen that the major contributions to energy levels nearest the HOMO-LUMO gap arise from the gold

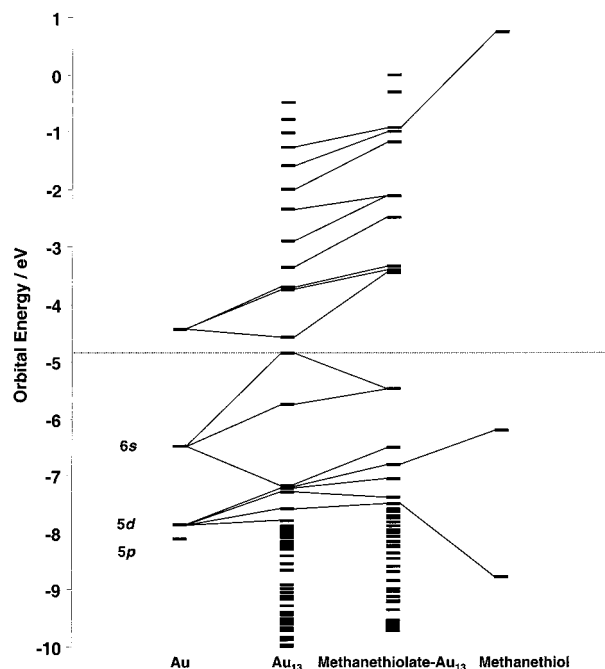


Figure 3. Molecular orbital energies of the Au atom (far left), Au₁₃ cluster (left), methanethiol (far right), and the methanethiolate-Au₁₃ complex (right), showing the composition of the molecular orbitals of the metal-molecule complex. The dashed horizontal line separates occupied and unoccupied energy levels.

TABLE 1: Composition of the Molecular Orbitals of the Methanethiolate-Au₁₃ Complex^a

MO	energy/eV	gold cluster	methanethiol
LUMO+7	-0.928 (a ₁)	6s band	S 3s 3p _y and C 2s 2p _y
LUMO+4	-2.133 (e)	6s band	S 3p _z
LUMO+3	-2.495 (a ₂)	6s band	S 3s
LUMO+2	-3.329 (a ₁)	6s band	
LUMO+1	-3.412 (e)	6s band	S 3p _z
LUMO	-3.451 (a ₁)	6s band	S 3s
HOMO	-5.483 (e)	6s band	S 3p _z
HOMO-1	-6.507 (a ₁)	6s band	S 3s
HOMO-2	-6.814 (e)	5d band	S 3p _z and H 1s
HOMO-3	-7.053 (a ₂)	5d band	
HOMO-4	-7.338 (e)	5d band	S 3p _z
HOMO-5	-7.508 (a ₁)	5d band	S 3s and C 2p _y

^a The contributions from the gold cluster are given in column two and the molecular contributions are given in column 3. A blank entry signifies that there is essentially no contribution to the molecular orbital from the fragment in question.

cluster 5d and 6s bands. The sulfur 3s contributions to the LUMO and HOMO-1 levels are small in comparison to the gold orbital contributions. The lowest molecular orbital of the molecule-cluster complex from which a molecular orbital of the thiolate molecule mixes strongly is the HOMO-2 level, which has a very strong contribution from the HOMO level of methanethiol, a predominately sulfur 3p_z state. The lowest molecular orbital of the complex into which the LUMO of methanethiol (sulfur 3s, 3p_y, and carbon 2s, 2p_y) mixes is LUMO+7. The energy gap between HOMO-2 and LUMO+7 is 5.89 eV, when compared to the HOMO-LUMO gap of the bare molecule of 6.94 eV indicates a narrowing between these molecular states upon bonding.

We have also considered the impact of constraining atomic positions, during the geometry optimization, on the electronic structure of the bonded complex. We fixed the gold cluster geometry and methanethiol geometry, and bonded these two sub-systems by fixing the sulfur-gold bond lengths to 2.500

TABLE 2: Mulliken Charges of the (111) Bonding Configuration of Methanethiolate–Au₁₃^a

atom	charge/electrons
S	−0.31
CH ₃	0.20
Au (bonded to S)	0.28
Au (remainder)	−0.75

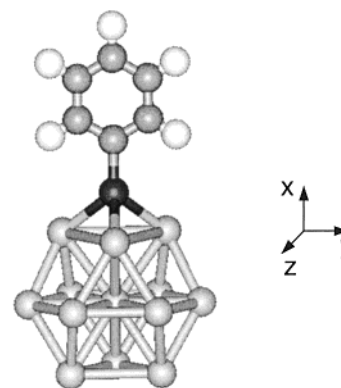
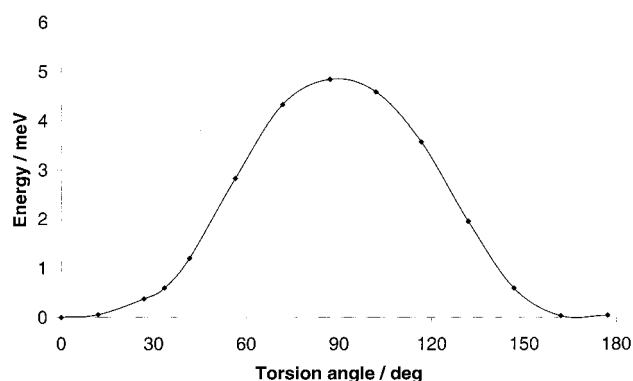
^a The notation (remainder) with respect to the gold charges is the sum of the atomic charges of the 10 gold atoms in the cluster not directly bonded to sulfur.

Å, close to the value for the relaxed structure. The resulting structure is termed the unrelaxed bonding configuration. Note that this constraint on the bonded system differs from previous studies whereby all gold atoms are constrained to their ideal bulk positions, with all neighboring gold–gold bonds frozen to 2.88 Å.^{4–6} The most important finding of our constrained studies is that the lack of geometry relaxation results in a HOMO–LUMO gap, which is significantly smaller than for the fully relaxed configuration. The HOMO–LUMO gap of the unrelaxed bonding configuration is 1.37 eV, while for the fully relaxed bonding configuration it is 2.03 eV, an increase of 0.66 eV. The energy of the LUMO is most affected, increasing by 0.41 eV, while the energy of the HOMO decreases by 0.24 eV. The shift in energy of other occupied and unoccupied orbitals is generally less than 0.2 eV, relative to the relaxed bonding configuration.

4.1.3. Charge Transfer. Mulliken population analysis was performed in order to examine the atomic charges of the methanethiolate–gold cluster complex. The atomic partial charges for the complex are given in Table 2. The charge on the sulfur atom within the free methanethiol is −0.11 electrons; bonding of methanethiolate onto the gold cluster results in an excess charge of 0.31 electrons on the sulfur atom. The magnitude of the charge on sulfur is in reasonable agreement with previous studies, where Sellers et al. find a charge of 0.40 electron (MBPT2/DZ) on sulfur,⁴ and Beardmore et al. find a charge of 0.42 electron (B-LYP/6-31G*) on the sulfur atom.⁵ The discrepancies in the calculated atomic charges on sulfur can be attributed to the fact that different theoretical methods and the differing basis sets used in the various studies give rise to variation in the charge analysis.

4.2. Benzenethiolate–Au₁₃. The study of the interaction between benzenethiol and gold is of importance as the benzenethiolate–gold complex is currently considered the prototypical system for transport studies in molecular electronics. For the minimum energy configuration for benzenethiolate bonded to the Au₁₃ cluster, the sulfur atom is bonded at a (111) hollow site as shown in Figure 4.

4.2.1. Bonding Configurations. Calculated bond lengths and bond angles for the complex are as follows: the sulfur–carbon bond distance is 1.795 Å. The distance from sulfur to the out-of-plane (with respect to the C_s mirror plane; see Figure 4) bonding gold atoms is 2.548 Å, and the distance to the in-plane gold atom is 2.599 Å. The bond distances from the central gold atom of the cluster to the out-of-plane bonding gold atoms are 3.098 Å and to the in-plane gold atom is 3.175 Å. These two bond lengths are 0.169 Å (5.8%) and 0.246 Å (8.4%) longer as compared to the same bond in the bare gold cluster. The bond lengths of the bonding gold atoms out of plane to the in-plane bonding gold atom is 3.667 Å, and the bond distance between the two out-of-plane bonding gold atoms is 3.580 Å. These bond lengths are 0.738 Å (25%) and 0.651 Å (22%) longer than the gold–gold bond lengths in the bare metal cluster. The distances from the central gold atom to the other atoms of the cluster are

**Figure 4.** Molecular structure of the (111) bonding configuration of benzenethiolate–Au₁₃ in C_s symmetry.**Figure 5.** Energy as a function of torsion angle about the sulfur–carbon bond in benzenethiolate–Au₁₃. The horizontal axis is the torsion angle in degrees and the vertical axis is the energy relative to the optimum torsion angle in milli-electronvolts.

all approximately 2.936 Å (within 0.007 Å to the bond length found for the bare Au₁₃ cluster), again indicating that only the gold bonds directly involved in bonding to the thiolate undergo substantial distortion. The carbon–carbon bond lengths in the ring are between 1.398 and 1.404 Å. The plane of the phenyl ring forms an angle of 4.2° with the normal of the gold plane.

We have investigated the energy barrier for rotation of the phenyl ring about the sulfur–carbon bond within the benzenethiolate–gold complex. This aspect of the benzenethiolate–gold bonding geometry was studied by carrying out single point calculations at different values of the torsion about the sulfur–carbon bond and the resulting energies are shown within Figure 5. It is seen from the magnitude of the energy barrier that the ring is essentially free to rotate about the sulfur–carbon bond at room temperature.

4.2.2. Electronic Structure. Within Figure 6, single particle energy levels of the gold atom, the gold cluster, the benzenethiol molecule, and the benzenethiolate–gold cluster complex are presented. Similar to our findings for the methanethiolate–gold complex, the HOMO–LUMO levels of the benzenethiolate–Au₁₃ complex are constructed largely from the HOMO–LUMO of the gold cluster. The primary contributions to the molecular orbitals of the benzenethiolate–Au₁₃ complex are identified within Table 3. As for the methanethiolate–Au₁₃ complex, the major contributions to energy levels near in energy to the HOMO–LUMO states of the benzenethiolate–Au₁₃ complex are from gold cluster states derived from 5d and 6s bands. HOMO-2 of the complex is the first energy level of the complex into which a molecular orbital derived from the thiol molecule mixes strongly, this corresponding to the HOMO of the thiol molecule. Additionally, the HOMO of benzenethiol mixes

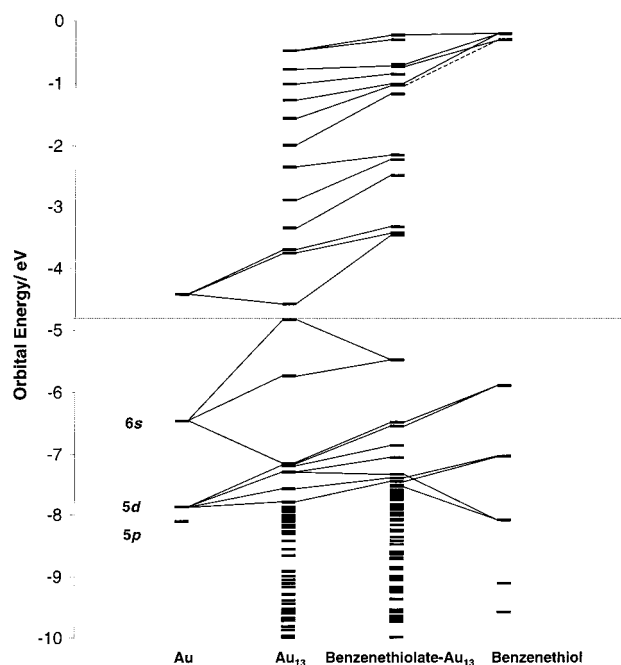


Figure 6. Molecular orbital energies of the Au atom (far left), Au₁₃ cluster (left), benzenethiol (far right), and the benzenethiolate–Au₁₃ complex (right), showing the composition of the molecular orbitals of the metal–molecule complex. The dashed horizontal line separates occupied and unoccupied energy levels and the dashed connection line indicates a small contribution from the LUMO of benzenethiol.

TABLE 3: Composition of the Molecular Orbitals of the Benzenethiolate–Au₁₃ Complex^a

MO	energy/eV	gold cluster	methanethiol
LUMO+14	−0.203 (a')	6s band	S 3p _z and C 2p _z
LUMO+13	−0.315 (a'')	6s band	
LUMO+12	−0.702 (a')	6s band	S 3p _z and C 2p _z
LUMO+11	−0.752 (a'')		C 2p _z
LUMO+10	−0.869 (a')	6s band	
LUMO+4	−2.506 (a'')	6s band	
LUMO+3	−3.336 (a')	6s band	S 3s
LUMO+2	−3.429 (a'')	6s band	S 3p _x
LUMO+1	−3.439 (a')	6s band	S 3p _z
LUMO	−3.468 (a')	6s band	S 3s
HOMO	−5.485 (a')	6s band	S 3p _z
HOMO-1	−5.489 (a'')	6s band	S 3p _x
HOMO-2	−6.489 (a')	6s band	S 3p _z and C 2p _z
HOMO-3	−6.557 (a')	5d band	S 3p _z and C 2p _z
HOMO-4	−6.870 (a'')	5d band	S 3p _x
HOMO-5	−7.064 (a'')	5d band	
HOMO-6	−7.344 (a')	5d band	S 2p _z and C 2p _z
HOMO-7	−7.411 (a'')	5d band	S 3p _z and C 2p _z
HOMO-8	−7.467 (a'')		C 2p _z

^a The contributions from the gold cluster are given in column two and the molecular contributions are given in column 3. A blank entry signifies that there is essentially no contribution to the molecular orbital from the fragment in question.

strongly with the cluster orbitals to give HOMO-3 of the complex. For HOMO-2 and HOMO-3 of the metal–molecule complex, the sulfur–gold interaction is of a bonding nature with an antibonding interaction between the sulfur and the phenyl ring. The above discussion is clarified by consideration of Figure 7a–c, in which are displayed the molecular orbitals of the HOMO, HOMO-2, and HOMO-3 of the benzenethiolate–Au₁₃ complex. Figure 7a shows the dominant gold 6s contribution to the HOMO of the complex. Figure 7, parts b and c, show clearly the strong contributions of the π -orbitals on the benzene ring and the sulfur atom to HOMO-2 and HOMO-3. This is in addition to the gold contribution. We postulate these orbitals

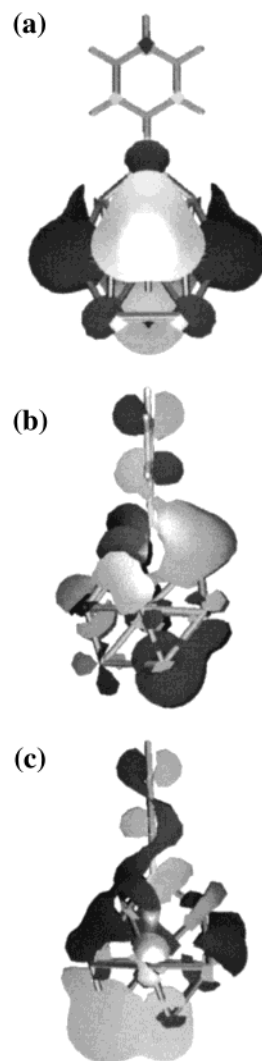


Figure 7. (a) Highest occupied molecular orbital (HOMO), (b) HOMO-2, and (c) HOMO-3 of the benzenethiolate–Au₁₃ complex.

could be of importance for resonant tunneling through the benzenethiol molecule. Regarding the low-lying unoccupied molecular orbitals, those presented in Table 3 show almost exclusively gold character; in agreement with findings given in ref 6. The lowest unoccupied molecular orbital into which orbitals of the thiol molecule mix is LUMO+11 at −0.75 eV, where the interaction is between the benzenethiol LUMO and the gold 6s band, giving antibonding character on the ring, no sulfur contribution, and a bonding ring–gold interaction. Additionally LUMO+12 and LUMO+14 also have a strong interaction between the cluster and the molecule. The energy gap between HOMO-2 and LUMO+11 is 5.74 eV, as compared to the HOMO–LUMO gap of the bare molecule, which is 5.61 eV, indicating relatively little energy change upon bond formation to the gold cluster. The effect of geometry relaxation on the electronic structure was also examined for benzenethiolate–Au₁₃. Results similar to those for methanethiolate–Au₁₃ are found, in that the HOMO–LUMO gap increases, in this case by 0.62 eV, when the molecule–metal complex is fully relaxed.

An important concern for molecular transport studies is the position of the gold Fermi level, taken to lie in the half-filled 6s band, with respect to the HOMO–LUMO gap of the thiol. In some instances it has been assumed that the Fermi level (or HOMO for a finite cluster) of the gold lies in the middle of the HOMO–LUMO gap of the thiol molecule.¹² However, recent

TABLE 4: Mulliken Charges of the (111) Bonding Configuration of Benzenethiolate–Au₁₃^a

atom	charge/electrons
S	−0.26
C	0.09
benzene ring (rest)	0.05
Au (bonded to S)	0.25; 0.31
Au (remainder)	−0.69

^a For the table entry Au (bonded to S), we list the charges of the two out-of-plane gold atoms and the single in-plane gold atom. The notation (rest) of the benzene ring is the sum of the charges of the remainder of the carbon and hydrogen atoms in the ring. The notation (remainder) with respect to the gold charges is the sum of the atomic charges of the remaining 10 gold atoms in the cluster.

work from Yaliraki et al.,³ using Hartree–Fock (HF) methods and the calculations of Emberley and Kirczenow¹⁹ using Extended Hückel Theory (EHT), has suggested that the energy of the gold HOMO lies close to the energy of the HOMO of the organic molecule, for the cases of α,α' -xylyl dithiol³ and benzenethiol.¹⁹ DFT has been used in this work in order to obtain a better description of the unoccupied molecular orbitals, the metal orbitals, and their alignment with respect to one another, and to investigate the above-mentioned relative position of the Fermi level. The HOMO–LUMO gap of the metal–molecule system is also much smaller than for the molecule itself, due to the appearance of levels (mostly of metallic origin) in the molecular HOMO–LUMO gap. Seminario et al.²⁰ have studied transport through a proposed molecular resonant tunneling diode (RTD). Fundamental assumptions made in their work are that the HOMO–LUMO gap gives a qualitative indication of the ability of a molecule to conduct, and that conduction is assumed to occur predominantly through the molecular LUMO. The small shift of the “molecular” HOMO–LUMO gap when bonded to Au₁₃, at least for benzenethiol (HOMO-2 and LUMO+11), encourages this approximation. On the other hand, it has been suggested that transport is expected to take place through orbitals other than solely the molecular LUMO, since previous work using EHT has suggested that other MOs of the molecule couple to the metal through the sulfur atom,¹⁹ which is also found in this work. The use of DFT to identify single-particle energies is not without its own difficulties but is believed to be more representative than HF single-particle energies. The DFT calculations presented here can be taken to substantiate recent findings that the gold HOMO aligns itself closely to the energy of the HOMO of the organic molecule.

4.2.3. Charge Transfer. The Mulliken charges are displayed in Table 4. The charge on the sulfur atom in benzenethiol is −0.09 electrons and upon bonding with the gold cluster, an excess charge of −0.26 electrons is found on the sulfur atom. A similar result was also found for benzenethiolate bonded to a 10-atom gold cluster in ref 6, with a charge excess of 0.20 electrons reported on the sulfur atom. The overall charge transfer to the thiol from the gold cluster is −0.12 electrons.

5. Conclusions

In this work we have considered the bonding of single thiolate molecules, to an ordered nanocluster, Au₁₃. The calculations reveal that thiolate bonding, even for these small structures, is in many aspects similar to bonding to gold surfaces and to larger gold clusters. The resulting bond distortions for bonding to (111) Au surfaces is similar in all cases: bulk surfaces, mesoscopic clusters, and to clusters consisting of a few atoms. Our calculations have been analyzed to determine the nature and

ordering of the single particle energy levels formed when the thiolate molecules are bonded to the Au₁₃ cluster.

We have shown upon bonding of the thiolate molecules to the gold cluster, the gold–gold bond lengths, for those gold atoms bonded to sulfur, elongate by 24% for methanethiolate and up to 25% for benzenethiolate. This effect is in agreement with the calculated results for methanethiolate bonded to the (111) gold surface using a slab model in ref 7, but in contrast to cluster model calculations used to describe bonding to the gold surface.^{4–6} Grönbeck et al. suggest the difference between the results from periodic slab models and cluster surface models indicates that clusters used in previous studies were too small to adequately describe thiolate–gold surface bonding. As our results obtained using a small, physical cluster agree with the slab model, our calculations suggest another reason for the discrepancies between previous calculations: to adequately describe thiolate bonding to gold surfaces and clusters, it is important to allow for relaxation of several layers of gold atoms. We are thus led to suggest the geometry constraints imposed on the cluster surface models applied in previous studies are too severe to allow for a proper quantitative description of thiolate bonding to gold. The bond length changes are less for the gold atoms not bonded directly to sulfur, but constraining atoms during the geometry optimization excludes the relaxation effects necessary for an accurate prediction of the local properties of thiolate–gold bonding.

The explicit nature of the coupling between thiol molecules and Au₁₃ has been presented in our work. Some work regarding the bonding between thiol molecules and gold has been performed previously using extended Hückel or Hartree–Fock methods,^{3,19} but the use of DFT methods allows for, although not a rigorous interpretation, a better subjective treatment of single particle energy levels, particularly for the unoccupied levels. Strong coupling between the gold cluster/thiol molecules has been highlighted for those molecular orbitals with a strong metal and thiol molecule character. Such levels are essential for resonant tunneling and for the usage of the molecules (thiolates) to be interpreted as “molecular wires”.

The HOMO of the gold cluster lies closer in energy to the HOMO than the LUMO of the organic molecule. The HOMO and LUMO of metal–molecule complexes are predominantly gold in character. High-lying occupied orbitals in methanethiolate–Au₁₃ show metal–sulfur coupling. High-lying occupied orbitals in benzenethiolate–Au₁₃ show strong metal–sulfur–molecule coupling. The LUMO of the bare molecule is lowered in energy upon interaction with the metal cluster and mixes with the gold orbitals at this lower energy. The value of the molecular HOMO–LUMO gap changes more significantly for the methanethiolate–gold than for the benzenethiolate–gold complex, upon interaction with the gold cluster. The change in the HOMO–LUMO gap of the thiol molecule and the offset of the gold 6s band and the molecular HOMO determined in this work substantiate similar findings from previous studies using extended Hückel and Hartree–Fock methods.^{3,6,19} The effect of geometry relaxation on the resulting electronic structure has been shown through a comparison of the energy levels of unrelaxed and relaxed thiolate–metal complexes. The HOMO–LUMO gap of the metal–molecule complex increases by 0.65 eV upon relaxation of the geometry of methanethiolate–Au₁₃, and by 0.62 eV for the benzenethiolate–Au₁₃ complex. We find relatively little change in the local character of the gold–sulfur bonds or the electronic structure of the thiolate–gold cluster when bonding either methane or benzene via the thiol linker. The bond lengths and bond angles are similar in both cases.

Hence, the sulfur atom largely determines the bonding to gold and it appears that the type of organic molecule that is attached to the sulfur is of minor importance to the bonding. The energy levels in the bonded complex corresponding to the molecular HOMO and LUMO undergo shifts in energy for both methanethiol and benzenethiol.

Charge transfer from the metal to the molecule was examined through Mulliken population analysis. A transfer of charge from the gold to the sulfur atom of the thiolate was clearly seen. The organic components of both metal–molecule complexes studied have an overall charge of about -0.1 electrons, giving an indication of the magnitude of the surface dipole produced upon bonding. Previous computational studies of electron transport across thiol attached molecules typically obtain conductances which are off by orders of magnitude when compared to experimental findings. It has been found that increasing the sulfur–gold distance to unphysical distances lead to better agreement with experimental values.¹⁹ Although in this work we do not obtain exaggerated sulfur to gold distances, it might be possible that the elongated gold–gold bond lengths obtained in the present study and the resulting increase in the HOMO–LUMO gap may improve theoretically predicted conductances relative to measured values.

Acknowledgment. This work has been funded by the European Union through the Information Society's Technology (IST) Program, within the Future and Emerging Technologies Advanced Research Initiative's NANOTCAD Project (IST-1999-10828), and the Improving Human Potential (IHP) Research Training Network (RTN) ATOMCAD (HPRN-CT-2000-00028).

References and Notes

(1) Reed, M. A.; Zhou, C.; Muller, C. J.; Burgin, T. P.; Tour, J. M. *Science* **1997**, 278, 252.

- (2) Chen, J.; Reed, M. A.; Rawlett, A. M.; Tour, J. M. *Science* **1999**, 286, 1550.
- (3) Yaliraki, S. N.; Roitberg, A. E.; Gonzalez, C.; Mujica, V.; Ratner, M. A. *J. Chem. Phys.* **1999**, 111, 6997.
- (4) Sellers, H.; Ulman, A.; Shindman, Y.; Eilers, J. E. *J. Am. Chem. Soc.* **1993**, 115, 9389.
- (5) Beardmore, K. M.; Kress, J. D.; Gronbeck-Jensen, N.; Bishop, A. R. *Chem. Phys. Lett.* **1998**, 286, 40.
- (6) Johansson, A.; Stafström, S. *Chem. Phys. Lett.* **2000**, 322, 301.
- (7) Grönbeck, H.; Curioni, A.; Andreoni, W. *J. Am. Chem. Soc.* **2000**, 122, 3839.
- (8) Akinaga, Y.; Nakajima, T.; Hirao, K. *J. Chem. Phys.* **2001**, 114, 8555.
- (9) Häkkinen, H.; Barnett, R. N.; Landman, U. *Phys. Rev. Lett.* **1999**, 82, 3264.
- (10) Garzón, I. L.; Rovira, C.; Michaelian, K.; Beltrán, M. R.; Ordejón, P.; Junquera, J.; Sánchez-Portal, D.; Artacho, E.; Soler, J. M. *Phys. Rev. Lett.* **2000**, 85, 5250; Garzón, I. L.; Artacho, E.; Beltrán, M. R.; García, A.; Junquera, J.; Michaelian, K.; Ordejón, P.; Rovira, C.; Sánchez-Portal, D.; Soler, J. M. *Nanotechnology* **2001**, 12, 126.
- (11) Häberlen, O. D.; Chung, S.-C.; Stener, M.; Rösch, N. *J. Chem. Phys.* **1997**, 106, 5189.
- (12) Samanta, M. P.; Tian, W.; Datta, S.; Henderson, J. L.; Kubiak, C. P. *Phys. Rev.* **1996**, B53, 7626.
- (13) Becke, A. D. *J. Chem. Phys.* **1993**, 93, 5486.
- (14) Lee, C.; Yang, W.; Parr, R. G. *Phys. Rev.* **1988**, B37, 785.
- (15) Ahlrichs, R.; Bär, M.; Häser, M.; Horn, H.; Kölmel, C. *Chem. Phys. Lett.* **1989**, 162, 165.
- (16) Cohen, A.; Handy, N. C. *Chem. Phys. Lett.* **2000**, 316, 160.
- (17) Andre, D.; Häussermann, H.; Dolg, M.; Stoll, H.; Preuss, H. *Theor. Chim. Acta* **1990**, 77, 123.
- (18) Schafer, A.; Horn, H.; Ahlrichs, R. *J. Chem. Phys.* **1992**, 97, 2571. Schafer, A.; Huber, C.; Ahlrichs, R. *J. Chem. Phys.* **1994**, 100, 5829.
- (19) Emberley, E.; Kirczenow, G. *Phys. Rev.* **1998**, B58, 10911.
- (20) Seminario, J. M.; Zacharias, A. G.; Tour, J. M. *J. Am. Chem. Soc.* **2000**, 122, 3000.